10Z-Hymenialdisine inhibits angiogenesis by suppressing NF-κB activation in pancreatic cancer cell lines

GORO UEDA[1], YOICHI MATSUO[1], HIROMICHI MURASE[1], YOSHINAGA AOYAMA[1], TOMOKATSU KATO[1],
KAN OMI[1], YUICHI HAYASHI[1], HIROYUKI IMAFUJI[1], KENTA SAITO[1], KEN TSUBOI[1,2], MAMORU MORIMOTO[1],
RYO OGAWA[1], HIROKI TAKAHASHI[1], AKIRA MITSUI[3], MASAHIRO KIMURA[2] and SHUJI TAKIGUCHI[1]

[1]Department of Gastroenterological Surgery, Nagoya City University Graduate School of Medical Sciences and
Medical School, Mizuho-cho, Mizuho-ku, Nagoya, Aichi 467-8601; [2]Department of Gastrointestinal Surgery,
Nagoya City East Medical Center, Chikusa-ku, Nagoya, Aichi 464-8547; [3]Department of Gastroenterological Surgery,
Nagoya City University West Medical Center, Kita-ku, Nagoya, Aichi 462-8508, Japan

Abstract. 10Z-Hymenialdisine is a natural product derived from the marine sponge *Axinella carteri*. 10Z-Hymenialdisine has anti-inflammatory effects exerted through NF-κB; however, it is unclear whether 10Z-Hymenialdisine has anti-angiogenic effects in cancer cells. In the present study, both the anti-angiogenic and antimetastatic effects of this compound in pancreatic cancer were investigated. It was initially confirmed that 10Z-Hymenialdisine significantly inhibited the proliferation of pancreatic cancer cells. Next, using both reverse transcription-quantitative PCR and ELISA, it was demonstrated that 10Z-Hymenialdisine significantly suppressed the expression of VEGF and IL-8 mRNAs and proteins in pancreatic cancer. Immunohistochemical analysis revealed that 10Z-Hymenialdisine inhibited NF-κB activity in pancreatic cancer cell lines. It was also identified that 10Z-Hymenialdisine inhibited tube formation in EA.hy926 cells. *In vivo*, 10Z-Hymenialdisine significantly inhibited the growth of BxPC-3 pancreatic cancer cells that were subcutaneously injected into model mice. In conclusion, the present study demonstrated that 10Z-Hymenialdisine exerted anti-angiogenic effects by suppressing NF-κB activity and angiogenic factors, such as VEGF and IL-8, in pancreatic cancer cell lines. 10Z-Hymenialdisine has potential applications as a novel therapeutic agent for the treatment of pancreatic cancer.

Correspondence to: Professor Yoichi Matsuo, Department of Gastroenterological Surgery, Nagoya City University Graduate School of Medical Sciences and Medical School, 1 Kawasumi Street, Mizuho-cho, Mizuho-ku, Nagoya, Aichi 467-8601, Japan
E-mail: matsuo@med.nagoya-cu.ac.jp

Introduction

Pancreatic cancer is a particularly aggressive malignant tumor with high morbidity and mortality (1). In 2018, epidemiological research revealed that pancreatic cancer was the fourth leading cause of cancer-related deaths in Japan and the third leading cause of cancer-related deaths in USA, with an estimated 227,000 deaths per year worldwide (2-4). In 2019, there were >56,000 new cases of pancreatic cancer and 46,000 pancreatic cancer-related deaths in the USA alone (3). Furthermore, pancreatic cancer is predicted to be the second leading cause of cancer-related deaths in USA by 2030 (5). Risk factors for pancreatic cancer include smoking, a family history of chronic pancreatitis, advanced age, occupational exposure, male sex, obesity, diabetes mellitus, a diet high in meat and low in vegetables and folate and a non-O blood group (6-8). The 5-year survival rate is <20%, even after radical surgery (6). Gemcitabine-based combination chemotherapy has been assessed for advanced pancreatic cancer. However, even with chemotherapy and radiotherapy, the effects are insufficient (6). Although numerous trials have been conducted to establish improved treatments for patients with advanced pancreatic cancer (S-1, oxaliplatin, fluorouracil and folic acid), no standard post first-line treatment has yet been identified (9-12). Thus, the development of new therapeutic options is urgently required.

The high malignancy of pancreatic cancer is due in part to constitutively activated NF-κB. NF-κB is a transcription factor that is associated with various functions, such as cell proliferation, inflammation and apoptosis. NF-κB is also involved in angiogenesis and metastasis in cancer, and enhances the production of angiogenic factors, such as VEGF and IL-8 (13,14). In our previous study the suppression of NF-κB signaling was found to decrease the production of both VEGF and IL-8 (15). It was confirmed that these factors are key mediators of angiogenesis and metastasis in pancreatic cancer (16-19). Furthermore, previous studies revealed that these factors support angiogenesis and are necessary for the metastasis of pancreatic cancer to the liver (20,21). Based on

these results, novel molecular therapies that target NF-κB are currently under development.

Certain natural products possess anti-inflammatory and anticancer effects against various cells and cancer types (22). Hymenialdisine, a natural product derived from the marine sponge *Axinella carteri* (*A. carteri*), has been reported to exhibit strong anti-inflammatory activity by suppressing NF-κB (23). Another study revealed that 10Z-Hymenialdisine inhibits the expression of IL-8 mRNA and protein in U937 cells (24). These data suggested that 10Z-Hymenialdisine may have potential anti-inflammatory and anti-angiogenic effects through NF-κB and various angiogenic factors, such as VEGF and IL-8 (24).

The anti-angiogenic effects of 10Z-Hymenialdisine in cancer cells have not been investigated. Therefore, in the present study, the effects of low-dose 10Z-Hymenialdisine on NF-κB activity, angiogenesis and metastasis in pancreatic cancer were examined. It was also investigated whether 10Z-Hymenialdisine prevents the production of angiogenic factors, such as IL-8 and VEGF. The anti-angiogenic effects of 10Z-Hymenialdisine were also evaluated *in vitro* and *in vivo*.

Materials and methods

Reagents. 10Z-Hymenialdisine and dimethyl sulfoxide (DMSO) were purchased from Sigma-Aldrich; Merck KGaA. Hymenialdisine was dissolved in DMSO to a stock concentration of 10 mM and stored at -20˚C.

Cell lines and cell culture. The three human pancreatic adenocarcinoma cell lines MIA PaCa-2 (cat. no. CRL-1420), SW 1990 (cat. no. CRL-2172) and BxPC-3 (cat. no. CRL-1687) and the immortalized human endothelial cell line EA.hy926 (cat. no. CRL-2922) were purchased from the American Type Culture Collection. MIA PaCa-2 and SW-1990 cells were cultured in DMEM and BxPC-3 cells were cultured in RPMI medium (both from Sigma Aldrich; Merck KGaA) in a 37˚C humidified incubator with 5% CO_2. These media were supplemented with 10% FBS, 10,000 U/ml penicillin, 25 μg/ml amphotericin B and 10 mg/ml streptomycin (all from Gibco; Thermo Fisher Scientific, Inc.).

Colony formation assay. Colony formation assays were performed using Diff-Quik solution (Sysmex Corporation). MIA PaCa-2, SW-1990 and BxPC-3 cells were seeded at $5x10^2$ cells into each well of a six-well plate and cultured for 1 day at 37˚C. The cells were then treated with various concentrations (0, 1, 2, 5 and 10 μM) of 10Z-Hymenialdisine. After 7 days of incubation at 37˚C, the plates were gently washed with PBS and subsequently stained with Diff-Quik solution, which included Diff-Quik fixative reagent for 5 sec, Diff-Quik solution I (eosinophilic) for 5 sec and Diff-Quik solution II (basophilic) for 5 sec, as designated in the manufacturer's protocol at room temperature. Colonies were determined to be formed when there were ≥50 cancer cells.

Cell proliferation assay. Cell proliferation assays were performed using a Premix WST-1 Cell proliferation Assay System (Takara Bio, Inc.) according to the manufacturer's protocol. MIA PaCa-2, SW-1990 and BxPC-3 cells were seeded at $2x10^5$ cells into each well of a 96-well plate to a total volume of 100 μl and cultured for 1 day at 37˚C. The cells were then treated with various concentrations (0, 1, 2, 5, 10 and 20 μM) of 10Z-Hymenialdisine and DMSO (equivalent to the concentration contained in 20 μM) at room temperature. After incubation for 72 h at 37˚C, absorbance was measured at 450 nm using a Spectra Max 340 spectrophotometer (Molecular Devices, LLC).

Immunocytochemistry for NF-κB. MIA PaCa-2, SW-1990 and BxPC-3 cells were seeded at $1x10^4$ cells/chamber in a four-chamber glass slide and cultured for 1 day at 37˚C. The cells were treated with 10Z-Hymenialdisine (5 μM) for 2 h at room temperature, followed by stimulation with TNF-α (1 ng/ml) for 20 min. Cells that had not been treated were used as controls. The cells were then washed with PBS and fixed with 4% paraformaldehyde for 20 min at room temperature. Next, the cells were washed with PBS, permeabilized with 0.1% Triton-X for 3 min, and incubated with 3% bovine serum albumin (BSA; FUJIFILM Wako Pure Chemical Corporation) for 1 h at room temperature. Subsequently, slides were treated with rabbit antibodies against NF-κB p65 (Cell Signaling Technology, Inc.; cat. no. 8242; 1:400) overnight at 4˚C and then treated with goat anti-rabbit IgG secondary antibodies H&L (Alexa Fluor® 488) (cat. no. ab150077; Abcam) for 1 h at room temperature. Primary and secondary antibodies were used at 1:400 and 1:500 dilution with 3% BSA, respectively. Cell nuclei were subsequently stained with DAPI (50 ng/ml) at room temperature for 10 min. Images of the stained slides were captured using a BZ-X710 fluorescent microscope at x400 magnification (Keyence Corporation).

Protein extraction and NF-κB activity assays. MIA PaCa-2, SW-1990 and BxPC-3 cells were seeded at $2x10^6$ cells/dish in 100-mm dishes and cultured for 1 day at 37˚C. The cells were treated with or without 10Z-Hymenialdisine (5 μM) for 2 h and then stimulated with or without TNF-α (1 ng/ml) for 20 min before the end of incubation. After the indicated treatment, nuclear protein was extracted using a Nuclear Extract Kit (Active Motif, Inc.) according to the manufacturer's protocol. The concentration of proteins in the nuclear extract was evaluated using a Pierce BCA Protein Assay kit (Thermo Fisher Scientific, Inc.) and stored at -80˚C until use. The activity of NF-κB was measured using a Trans AM NF-κB p65 Active Transcription Assay Kit (Active Motif, Inc.) according to the manufacturer's protocol. A total of 5 micrograms of nuclear extract protein was used in the NF-κB activity assay.

Reverse transcription-quantitative PCR (RT-qPCR). MIA PaCa-2, SW-1990 and BxPC-3 cells were seeded at $4x10^5$ cells/well in six-well plates containing medium (MIA PaCa-2 and SW-1990 cells were cultured in DMEM and BxPC-3 cells were cultured in RPMI medium) and cultured for 1 day at 37˚C. Then, the medium was changed, and the cells were cultured for an additional 2 h with or without 10Z-Hymenialdisine (5 μM) at 37˚C. Total RNA was extracted from cell pellets using an RNeasy Plus Mini Kit (Qiagen KK) according to the manufacturer's protocol and quantified using a Nano Drop 1000 spectrophotemer (Thermo Fisher Scientific,

Inc.) using 260 nm wavelength. Total RNA (1 μg) was reverse transcribed using Super Script III First-Strand Synthesis Super Mix for RT-qPCR kit (Invitrogen; Thermo Fisher Scientific, Inc.) according to the manufacturer's protocol. RT-qPCR was carried out using TaqMan Fast Advanced Master Mix (cat. no. 4444964; Thermo Fisher Scientific, Inc.) and TaqMan Gene Expression Assays for *IL-8* (Hs01553824_g1; cat. no. 4331182; Thermo Fisher Scientific, Inc.), *VEGF* (Hs00900055_m1; cat. no. 4331182; Thermo Fisher Scientific, Inc.) and *GAPDH* (Hs99999905_m1; cat. no. 4331182; Thermo Fisher Scientific, Inc.) with an Applied Biosystems 7900HT Fast Real-Time PCR System (Applied Biosystems; Thermo Fisher Scientific, Inc.). The thermocycling conditions for PCR were as follows: initial denaturation at 95˚C for 20 sec, followed by 40 cycles at 95˚C for 1 sec and 60˚C for 20 sec. The relative expression levels of *VEGF* and *IL-8* were normalized to the expression of *GAPDH* in each sample using the relative standard curve method (25).

ELISA analysis of IL-8 and VEGF levels. MIA PaCa-2, SW-1990 and BxPC-3 cells were seeded at $4x10^5$ cells/well in six-well plates containing medium (MIA PaCa-2 and SW-1990 cells were cultured in DMEM and BxPC-3 cells were cultured in RPMI medium) and cultured for 1 day at 37˚C. The culture medium was subsequently changed, and the cells were cultured for an additional 72 h at 37˚C in the presence of different concentrations of 10Z-Hymenialdisine (0, 1, 2 and 5 μM). After incubation, the culture medium was collected and centrifuged at 400 x g for 5 min at 14˚C to remove particles. The supernatants were frozen at -80˚C until use. The concentrations of IL-8 and VEGF were determined using human IL-8 (R&D Systems, Inc.; cat. no. D8000C) and human VEGF (R&D Systems, Inc.; cat. no. DVE00) ELISA kits according to the manufacturer's protocol.

Tube formation assays. Tube formation assays were conducted using EA.hy926 cells and Matrigel matrix (Corning Inc.) in the presence of the supernatants of pancreatic cancer cells. Cell supernatants were collected from the cancer cell culture medium (MIA PaCa-2 and SW-1990 cells were cultured in DMEM and BxPC-3 cells were cultured in RPMI medium) via centrifugation at 400 x g for 5 min at 14˚C. MIA PaCa-2, SW-1990 and BxPC-3 cells were seeded at $4x10^5$ cells/well in six-well plates containing medium (MIA PaCa-2 and SW-1990 cells were cultured in DMEM and BxPC-3 cells were cultured in RPMI medium) and cultured for 1 day at 37˚C. The culture media were then changed, and the cells were incubated for an additional 48 h at 37˚C in medium with or without 10Z-Hymenialdisine (5 μM), after which the supernatants were collected and centrifuged at 400 x g for 5 min at 14˚C to remove particles. EA.hy926 cells ($1.2x10^4$ cells/well) were seeded into each well of a 96-well plate coated with Matrigel. Matrigel was pre-coated for 30 min at room temperature. Then, the cells were cultured for 1 day at 37˚C with 50 μl 10% FBS and 50 μl of the aforementioned supernatant. Tube formation was observed by a BZ-X710 fluorescent microscope at x40 magnifications (Keyence Corporation) and evaluated by determining the number of the endotubes generated by EA.hy926 cells. A total of four random fields of view were analyzed per sample.

Animal studies. Female BALB/c nu-nu 12 mice (4 weeks old; weight range, 13-15 g) were purchased from Charles River Laboratories, Inc. The animals were housed in standard Plexiglas cages (maximum of 5 mice per cage) in a room maintained at constant temperature (20-26˚C) and humidity (40-60%) with a 12-h light/dark cycle. Mice were fed regular autoclaved chow and were provided water *ad libitum*. Anesthesia was administered by inhalation of isoflurane. Induction was conducted at 4-5% concentration and maintenance at 2-3%. Euthanasia was performed by cervical dislocation after adequate anesthesia. All experiments were conducted according to the Guidelines for Animal Experiments of Nagoya City University Graduate School of Medicine Sciences and were approved (approval no. Medical Animal 20-020) by the Animal Care and Use Committee of the Nagoya City University Graduate School of Medical Sciences (Nagoya, Japan).

Experimental protocol. BxPC-3 human pancreatic cells ($5x10^6$ cells in 100 μl PBS) were injected subcutaneously into the left flank of each mouse. Tumor volume was measured once a week using calipers. When the tumors reached a volume of ~50 mm^3, the mice were randomly divided into two groups (6 mice per group).

Mice in group I were administered DMSO (the same concentration as group II) diluted with PBS as a control, whereas mice in group II received intraperitoneal injections of 10Z-Hymenialdisine (10 mg/kg/week) diluted with PBS. The tumor volume was calculated according to the following formula: Tumor volume (mm^3)=(AxB^2)/2, where A and B represented the longest and shortest diameters in millimeters, respectively. Mice were injected intraperitoneally with DMSO or 10Z-Hymenialdisine once a week for 5 weeks and then sacrificed 1 week later. Finally, the tumors were excised and fixed in 10% formaldehyde at 4˚C for 24 h for further analysis.

Histopathological examination. Subcutaneous xenograft tumors were fixed with 4% paraformaldehyde at 4˚C for 6 h and embedded in paraffin. The sections (3 μm) were mounted on 3-amino-propyltriethoxysilane-coated slides. Dewaxed paraffin sections were placed in a microwave (10 min, 600 watts) to recover antigens before staining. The following antibodies (obtained from Cell Signaling Technology, Inc.) were used at 4˚C for 24 h: Rabbit monoclonal anti-Ki67 antibodies (cat. no. 9027; 1:500), mouse monoclonal anti-CD31 antibodies (cat. no. 3528; 1:1,000), rabbit monoclonal anti-NF-κB p65 antibodies (cat. no. 8242; 1:100). Biotin-conjugated secondary antibodies (all, Dako; Agilent Technologies, Inc) were also used at room temperature for 45 min: Anti-rabbit secondary antibodies (cat. no. K4003; 1:500) and anti-mouse secondary antibodies at room temperature for 45 min (cat. no. K4001; 1:1,500). Liqid DAB + Substrate Chromogen System (cat. no. K3467) were used as the chromogen for detection at room temperature for 10 min. Hematoxylin was used for nuclear counterstaining at room temperature for 30 sec.

For the quantification of NF-κB p65 activation, the number of nucleus-positive cells was counted. Nuclear translocation of p65 was considered to be a marker of NF-κB activation. Proliferation was quantified by determining the percentage of Ki67-positive cells. Results were expressed as the mean
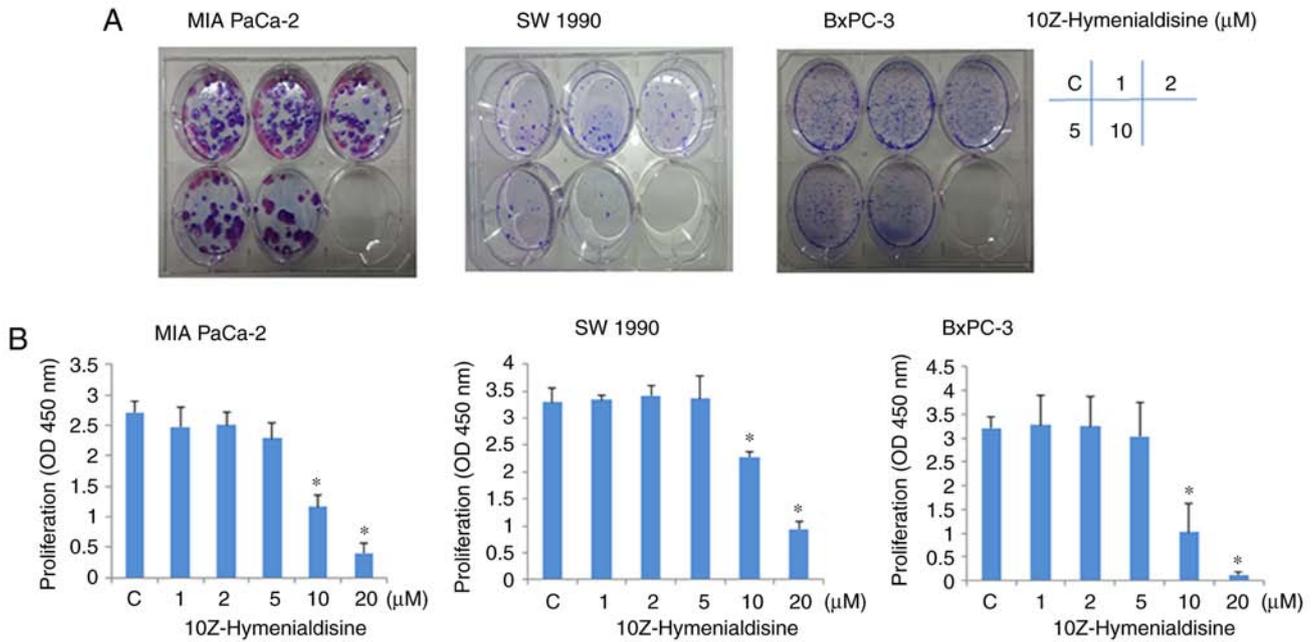
Figure 1. Effects of 10Z-Hymenialdisine on the proliferation of pancreatic cancer cell lines. Pancreatic cancer cell lines (MIA PaCa-2, SW-1990 and BxPC-3) were treated with 10Z-Hymenialdisine at the indicated concentrations for 72 h, after which cytotoxicity was measured using (A) colony formation and (B) WST-1 assays. Data are expressed as the mean ± SD (n=4). *P<0.05 vs. control. C, control.

number of Ki67-positive cells ± SD per high-power field. A total of three fields were examined from each tumor for each of the two treatment groups. For the quantification of microvessel density in sections stained for CD31, any distinct area of positive staining for CD31 was counted as a single vessel. Results were expressed as the mean number of vessels ± the SD per high-power field. A total of three random fields were examined and counted from each tumor for each of the two treatment groups. Images of the stained slides were captured using a BZ-X710 fluorescent microscope at x200 magnification (Keyence Corporation).

Statistical analysis. All experiments, except for *in vivo* procedures, were performed in triplicate. All experimental data are presented as the mean ± SD. Multiple group comparisons were performed using one-way ANOVA with Dunnett's post-hoc tests for subsequent individual group comparisons. Comparisons between two groups were performed using unpaired Student's t-tests. Comparisons between multiple groups with >1 reference group were analysed using Tukey's post hoc test. P<0.05 was considered to indicate a statistically significant difference. All statistical analyses were performed with EZR Version 1.54 (Saitama Medical Center, Jichi Medical University, Saitama, Japan), which is a modified version of R commander designed to add statistical functions frequently used in biostatistics (26).

Results

10Z-Hymenialdisine suppresses the proliferation of pancreatic cancer cell lines. Colony formation assays revealed that the growth of pancreatic cancer cell lines (MIA PaCa-2, SW-1990 and BxPC-3) was suppressed by 10Z-Hymenialdisine in a concentration-dependent manner (Fig. 1A). Consistent with

this, WST-1 assays revealed that 10Z-Hymenialdisine inhibited the proliferation of all three pancreatic cancer cell lines in a concentration-dependent manner, with significant inhibition observed at 10 μM (Fig. 1B). In subsequent experiments, to avoid cytotoxicity of 10Z-Hymenialdisine, the concentration of 10Z-Hymenialdisine was set at 5 μM.

10Z-Hymenialdisine inhibits the TNF-α-induced translocation of NF-κB. Immunocytochemical analysis revealed that p65 translocated into the nucleus of cells treated with TNF-α alone, whereas in cells treated with TNF-α and 10Z-Hymenialdisine (5 μM), p65 remained in the cytoplasm. The translocation of p65 into the nucleus was then examined using ELISA (Fig. 2A and B). The results demonstrated that 10Z-Hymenialdisine significantly decreased the translocation of p65 into the nucleus. This effect was confirmed with TNF-α. TNF-α alone significantly increased p65 translocation; however, the addition of 10Z-Hymenialdisine significantly decreased this effect (Fig. 2B).

10Z-Hymenialdisine decreases mRNA expression levels of IL-8 and VEGF. RT-qPCR revealed that 10Z-Hymenialdisine (5 μM) significantly decreased the mRNA expression levels of IL-8 and VEGF in pancreatic cell lines (Fig. 3A and B). In addition, ELISA revealed that the protein secretion levels of IL-8 and VEGF were reduced by 10Z-Hymenialdisine (1-5 μM; Fig. 4A and B). In the present experiment, all pancreatic cancer cell lines exhibited reduced levels of IL-8 and VEGF proteins in the presence of different concentrations of 10Z-Hymenialdisine (1-5 μM). For cells treated with 5 μM 10Z-Hymenialdisine, all pancreatic cancer cell lines demonstrated significant reductions in both IL-8 and VEGF. It was confirmed that the concentration of 5 μM was the most appropriate to inhibit angiogenic factors without causing cytotoxicity.
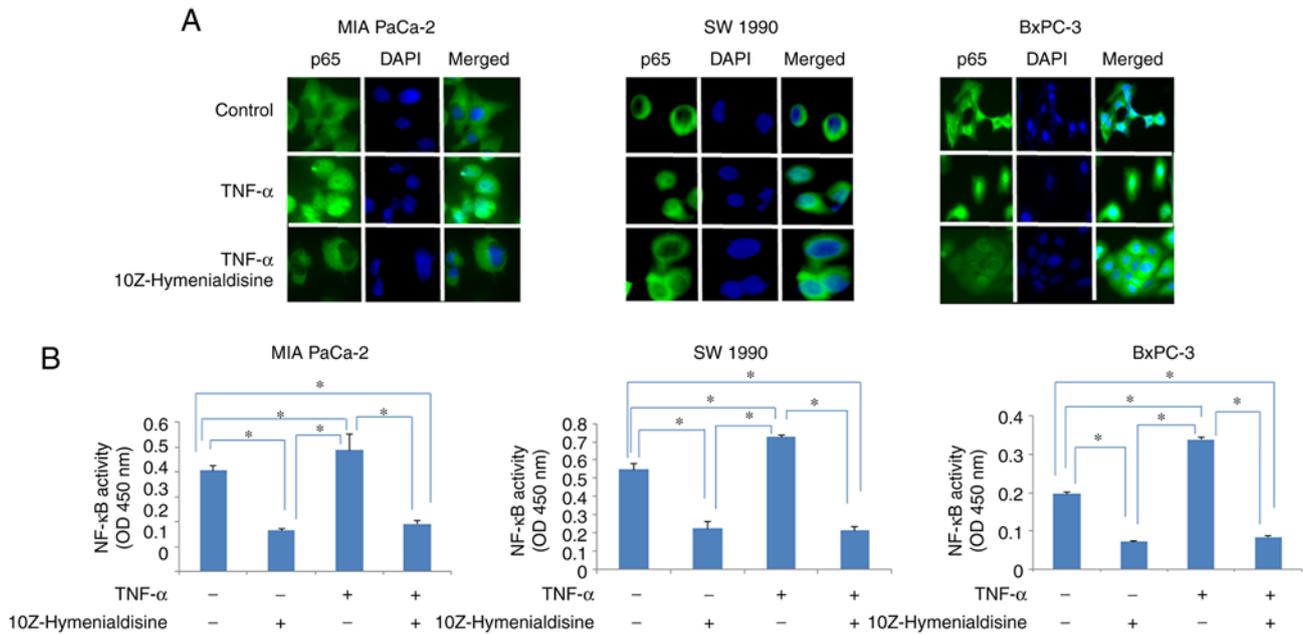
Figure 2. Effects of 10Z-Hymenialdisine on NF-κB activity in pancreatic cancer cell lines. Pancreatic cancer cell lines (MIA PaCa-2, SW-1990 and BxPC-3) were treated with 10Z-Hymenialdisine (5 μM) for 2 h and TNF-α (1 ng/ml) for 20 min. (A) Immunocytochemical analysis was used to assess the localization of NF-κB using antibodies against p65 (magnification, x400). (B) The activity of NF-κB in nuclear extracts was determined using ELISA. Values are expressed as the mean ± SD (n=4). *P<0.05 as indicated.
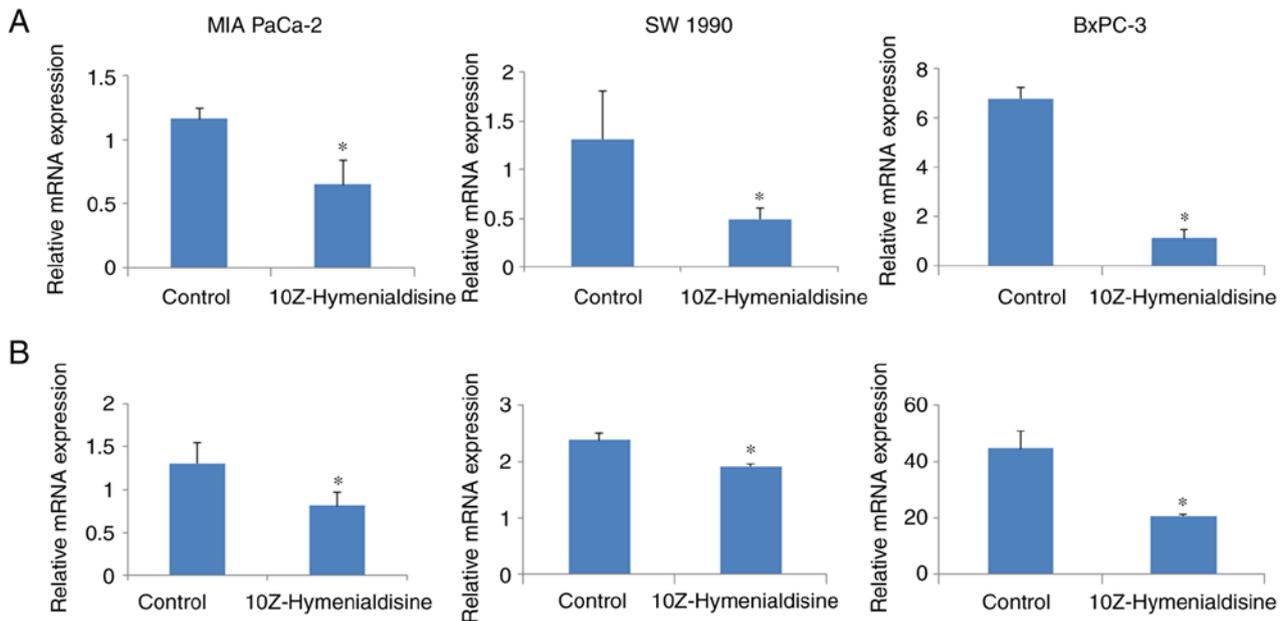

Figure 3. Effects of 10Z-Hymenialdisine on *IL-8* and *VEGF* mRNA expression in pancreatic cancer cells. Pancreatic cancer cell lines (MIA PaCa-2, SW-1990 and BxPC-3) were treated with 10Z-Hymenialdisine (5 μM) for 48 h. (A) *IL-8* and (B) *VEGF* mRNA levels were evaluated using reverse transcription-quantitative PCR (normalized to *GAPDH* expression). Values are expressed as the mean ± SD (n=4). *P<0.05 vs. control.

10Z-Hymenialdisine inhibits tube formation by human endothelial (EA.hy926) cells. Subsequently, tube formation assays were performed using human endothelial cells. Tube formation was enhanced when the cells were incubated with supernatants from untreated pancreatic cancer cell lines, but was significantly decreased when the cells were incubated with supernatants from 10Z-Hymenialdisine-treated pancreatic cancer cell lines (Fig. 5A). Tube formation was then evaluated by counting the number of endotubes. Endotube numbers

were significantly increased when the cells were incubated with supernatants from cancer cell lines and significantly decreased when the cells were incubated with supernatants from 10Z-Hymenialdisine-treated pancreatic cancer cell lines (Fig. 5B).

10Z-Hymenialdisine suppresses tumor growth in a subcutaneous xenograft model. BxPC-3 cells were subcutaneously injected into mice, after which tumors were allowed to
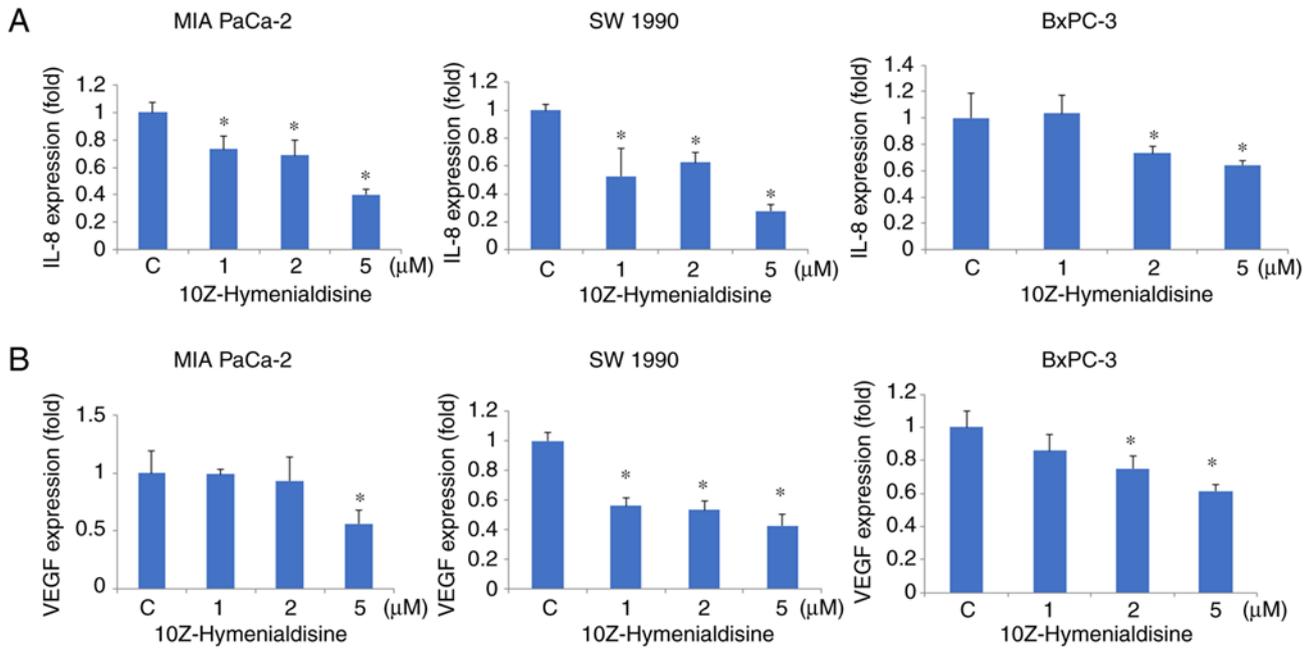
Figure 4. Effects of 10Z-Hymenialdisine on the secretion of IL-8 and VEGF by pancreatic cancer cell lines. Pancreatic cancer cell lines (MIA PaCa-2, SW-1990 and BxPC-3) were treated with 10Z-Hymenialdisine at the indicated concentrations for 72 h, after which the supernatants were collected. (A) IL-8 and (B) VEGF concentrations were determined using ELISA. Values are expressed as the mean ± SD (n=4). *P<0.05 vs. the control group. C, control.
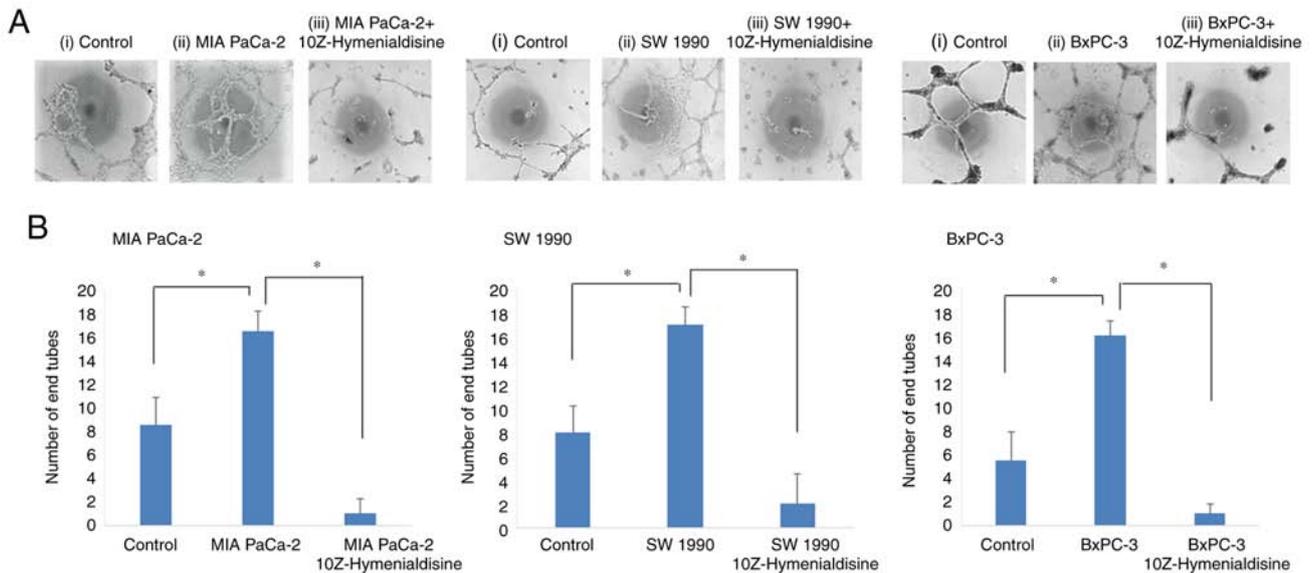

Figure 5. Effects of 10Z-Hymenialdisine on EA.hy926 pancreatic cancer cells induced to form tubes *in vitro*. EA.hy926 cells were cultured with control, supernatants of pancreatic cancer cell lines (MIA PaCa-2, SW-1990 and BxPC-3) and supernatants of pancreatic cancer cell lines treated with 10Z-Hymenialdisine (5 μM). (A) Representative images (magnification, x40): i) Control, ii) culture with supernatants from pancreatic cancer cell lines and iii) culture with supernatants from pancreatic cancer cell lines treated with 10Z-Hymenialdisine (5 μM). (B) The extent of tube formation by EA.hy926 cells. Values are expressed as the mean ± SD (n=4). *P<0.05 as indicated.

form. When the tumors had grown, mice were injected intraperitoneally with 10Z-Hymenialdisine (10 mg/kg) or DMSO for 5 weeks. One mouse in the control group succumbed in the middle of the treatment course owing to the maintenance 2-3% inhalation of isoflurane anesthesia. 10Z-Hymenialdisine significantly inhibited tumor growth 14 days after treatment (Fig. 6A-C). Body, liver and kidney weights were not decreased compared with those in the control group (Fig. 6D-F).

10Z-Hymenialdisine inhibits NF-κB (p65) activation, cell proliferation (Ki-67) and angiogenesis (CD31) in pancreatic cancer tumors. Resected pancreatic cancer tumors were evaluated using immunocytochemical analysis. It was revealed that p65 translocation into the nucleus was decreased in groups treated with 10Z-Hymenialdisine compared with the control group. To determine the effects of 10Z-Hymenialdisine on proliferation and angiogenesis, the expression of Ki-67, a cell proliferation marker, and CD31, a microvessel density marker,
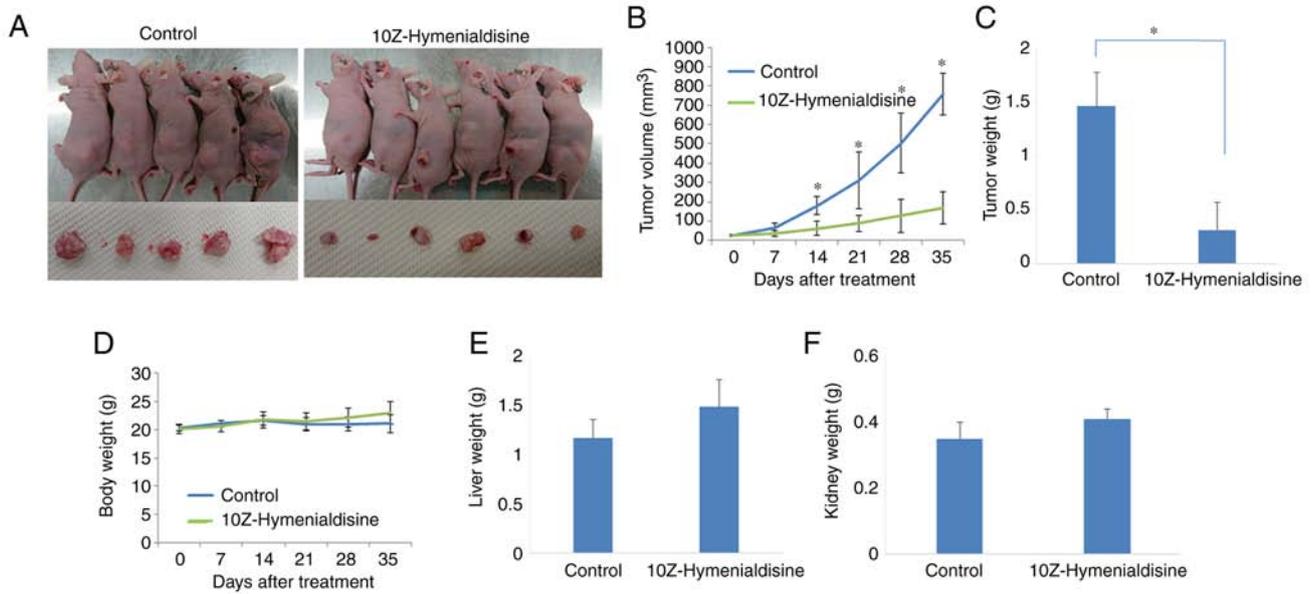
Figure 6. Effects of 10Z-Hymenialdisine on tumor growth in a subcutaneous xenograft model using BxPC-3 pancreatic cancer cells. Pancreatic cancer cells were subcutaneously injected and allowed to develop. Mice were then divided into two groups: Control (group I) and 10Z-Hymenialdisine (group II). The solution was injected intraperitoneally weekly for 5 weeks. Mice were sacrificed on week 6. (A) Images of the mice and excised tumors. (B) Tumor volumes were measured weekly. (C) Weights of the removed tumors at sacrifice. (D) Body weights in each group of mice were measured weekly. (E) Liver and (F) kidney weights were determined after sacrifice. Values are expressed as the mean ± SD. *P<0.05 vs. control.
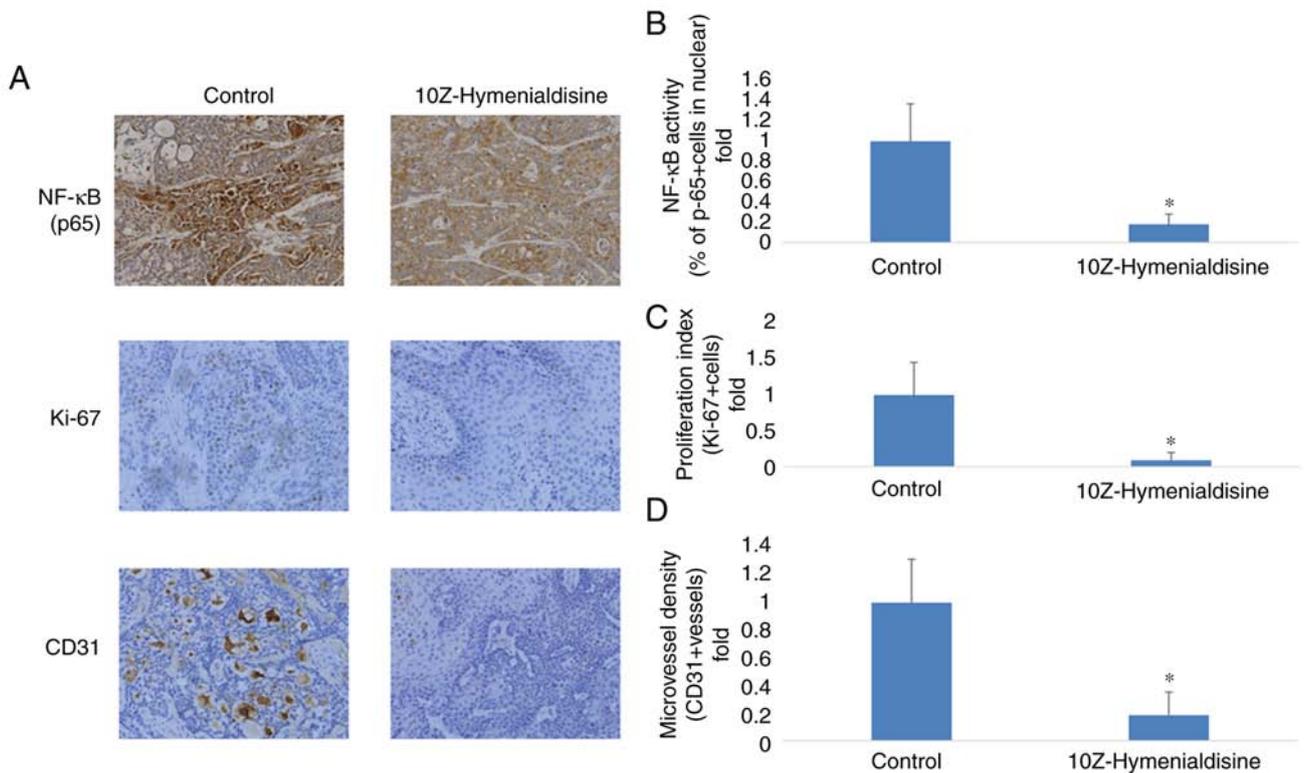

Figure 7. Effects of 10Z-Hymenialdisine on NF-κB (p65) activation, proliferation (Ki-67) and angiogenesis (CD31) in pancreatic cancer tumors. (A) Immunohistochemical analysis. Representative images are presented (magnification, x200). (B) Quantification of NF-κB (p65) activation. (C) Quantification of Ki-67-positive cells. (D) Quantification of microvessel density. Values in (B-D) are expressed as the mean ± SD. *P<0.05 vs. control.

were examined in tumor tissues. As demonstrated in Fig. 7, 10Z-Hymenialdisine significantly decreased the activation of NF-κB (p65) and inhibited the expression of Ki-67 and CD31 (Fig. 7A-D).

10Z-Hymenialdisine decreases mRNA expression levels of IL-8 and VEGF in pancreatic cancer tumors. The expression levels of targeted mRNAs in resected pancreatic cancer tumors were then evaluated using RT-qPCR. The results revealed
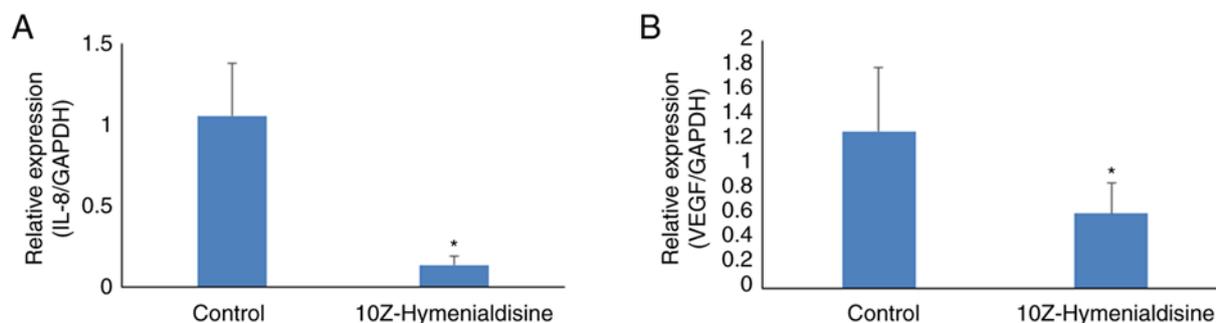
Figure 8. Effects of 10Z-Hymenialdisine on the expression of *VEGF* and *IL-8* in pancreatic cancer tumors. (A) *IL-8* and (B) *VEGF* mRNA levels were measured using reverse transcription-quantitative PCR (normalized to *GAPDH* expression). Values are expressed as the mean ± SD. *P<0.05 vs. control.

that 10Z-Hymenialdisine significantly decreased the mRNA expression levels of *IL-8* and *VEGF* in pancreatic cancer tumors compared with that in control tumors (Fig. 8A and B).

Discussion

10Z-Hymenialdisine is a natural product derived from the marine sponge *A. carteri*. In the present study, it was demonstrated that 10Z-Hymenialdisine inhibited the proliferation of pancreatic cancer cells, blocked NF-κB activity and suppressed the expression of the angiogenic factors VEGF and IL-8. In addition, 10Z-Hymenialdisine inhibited tube formation by EA.hy926 human endothelial cells. These experiments suggested that 10Z-Hymenialdisine may have potential applications as an anti-angiogenesis agent. Finally, using *in vivo* modeling, it was identified that 10Z-Hymenialdisine inhibited tumor growth by subcutaneously injecting BxPC-3 pancreatic cancer cells. In this model, no decrease was observed in body, liver, or kidney weights in the 10Z-Hymenialdisine-treated group of mice. Previous studies revealed that NF-κB has important roles in the regulation of apoptosis, oncogenesis and angiogenesis (27,28). Importantly, ~70% of pancreatic cancer cells exhibit constitutive activation of NF-κB (29). Furthermore, in certain studies, upregulation of NF-κB explains, at least in part, the resistance of cells to chemotherapy (30-33).

The aggressive growth and metastasis of pancreatic cancer is partly caused by its angiogenic capacity, which has been attributed to the release of angiogenic factors derived from tumors and stromal cells (34). Numerous angiogenic factors have been identified, among which VEGF and IL-8 are considered to be key mediators of angiogenesis in pancreatic cancer (16,18). Suppression of angiogenic factors would be a highly desirable effect of any new chemotherapeutic agent.

Given the relationship between NF-κB and certain angiogenic factors, such as VEGF and IL-8, suppressing the activity of NF-κB would be beneficial in treating pancreatic cancer. A previous study demonstrated that inhibition of NF-κB activity by the proteasome inhibitor MG132 decreases the expression of VEGF and IL-8 and inhibits tumor-induced angiogenesis (15). The experiments of the present study were consistent with these previous studies. It was demonstrated that 10Z-Hymenialdisine inhibited tube formation by EA.hy926 human endothelial cells. Thus, the data revealed that 10Z-Hymenialdisine suppressed the expression of VEGF and IL-8 via inhibition of NF-κB activity in pancreatic cancer

cell lines. As a result, 10Z-Hymenialdisine inhibited tube formation by human endothelial cells.

The anti-angiogenic effects of bortezomib, an NF-κB inhibitor, have been exploited for the treatment of patients with multiple myeloma (35); however, this NF-κB inhibitor has strong side effects, and adoption of such chemotherapeutic agents is not widely accepted (35). Consequently, new NF-κB inhibitors with low non-specific toxicity are urgently needed.

In Nagoya City University Graduate School of Medical Sciences and Medical School, the Department of Gastroenterological Surgery's laboratory, focus has been addressed on natural products. Natural agents, such as escin, curcumin, sesamin, xanthohumol and zerumbone, have been shown to have anticancer effects (22,36-40). Previous studies have demonstrated that these natural products inhibit NF-κB and certain angiogenic factors, such as VEGF and IL-8, and exhibit efficacy in *in vivo* models (39,40). Xanthohumol exerts anticancer effects without causing body weight changes in mice (40). Furthermore, curcumin, a natural product, can be used in combination with gemcitabine to inhibit the activity of NF-κB and exert synergistic effects on tumor suppression (41). Accordingly, 10Z-Hymenialdisine may have applications as a combination therapy with existing anticancer agents, such as gemcitabine, to further enhance the anticancer effects of the treatment, similar to curcumin. Previous studies have revealed that 10Z-Hymenialdisine inhibits NF-κB and various cytokines, including IL-1, IL-2, IL-8 and TNF-α in certain types of cells (24,42). Additionally, 10Z-Hymenialdisine has been reported to have anticancer effects (43); however, this is the first report, to the best of our knowledge, demonstrating that 10Z-Hymenialdisine exerts inhibitory effects on pancreatic cancer cells by suppressing NF-κB and angiogenesis.

To assess the cytotoxic effects of 10Z-Hymenialdisine, colony formation and cell proliferation assays were conducted. Since previous studies revealed that 10Z-Hymenialdisine is active at concentrations of 1-10 μM, these concentrations were initially examined (23,24). In the latter experiment, 10Z-Hymenialdisine showed cytotoxic effects at high concentrations (>10 μM). In subsequent experiments, to confirm the anti-angiogenic effects of 10Z-Hymenialdisine, the experiments were primarily conducted using low concentrations (≤5 μM), which did not suppress cell proliferation. At low concentrations (≤5 μM), 10Z-Hymenialdisine inhibited the activity of NF-κB and blocked the expression of VEGF and IL-8. 10Z-Hymenialdisine also inhibited tube formation. Thus,

it was concluded that 10Z-Hymenialdisine may have potential clinical applications via suppression of angiogenesis, without causing substantial cytotoxicity.

In terms of angiogenesis, pancreatic cancer is generally considered to be a type of ischemic tumor, and vessel densities are low in imaging; however, angiogenesis is associated with prognosis in patients with pancreatic cancer (44-46), and certain studies have demonstrated that anti-angiogenic treatments exhibit favorable efficacy in pancreatic cancer (47,48). Similarly, to ensure that the findings of the present study provided an adequate reflection of pancreatic cancer, experiments were conducted using three different pancreatic cancer cell lines [MIA PaCa-2 (undifferentiation, with *KRAS* mutation), SW-1990 (high/moderate differentiation, with *KRAS* mutation) and BxPC-3 (moderate differentiation, without *KRAS* mutation)]. In all *in vitro* experiments, these three pancreatic cancer cell lines showed similar trends with regard to the effects of 10Z-Hymenialdisine.

In the mouse experiments of the current study, the suppression of tumor growth by 10Z-Hymenialdisine was demonstrated. No previous studies have described the use of 10Z-Hymenialdisine in such *in vivo* models. Therefore, it remains necessary to optimize the dosage and administration method for 10Z-Hymenialdisine. It was previously identified that another natural product, xanthohumol, inhibits pancreatic cancer growth (40). Xanthohumol has a molecular weight similar to that of 10Z-Hymenialdisine, and its anticancer effects are achieved at a similar concentration (10 mg/kg) *in vitro*. Based on these findings, the appropriate concentration and administration method for 10Z-Hymenialdisine was selected; however, further studies are required to optimize its use.

In conclusion, the results of the present study demonstrated that 10Z-Hymenialdisine inhibited angiogenesis by suppressing NF-κB activity in pancreatic cancer cell lines. This effect was achieved by blocking the expression of various angiogenesis factors, such as IL-8 and VEGF. The anti-angiogenic effects of 10Z-Hymenialdisine were also demonstrated using EA-hy926 human endothelial cells. Finally, it was revealed that 10Z-Hymenialdisine had anticancer effects in a mouse model. These effects were obtained at relatively low concentrations that did not exhibit cytotoxicity. Furthermore, there was no body weight loss or other organ weight loss. As with the majority of studies, the design of the current study is subject to some limitations. For example, it was not known where and how 10Z-Hymenialdisine acts on the NF-κB pathway. Furthermore, the animal experiment was performed using the subcutaneous injection of pancreatic cancer cells, which is different from actual pancreatic cancer. Therefore, the results of the animal experiment cannot be directly applied to humans. So further investigation is required, such as orthotopic cancer model *in vivo* experiments. However, 10Z-Hymenialdisine could be a potential therapeutic agent for pancreatic cancer.

Availability of data and materials

The data generated or analyzed during this study are included in the published article.

Authors' contributions

GU and YM contributed to the conception and design of the study, analyzed and interpreted the data and wrote and reviewed the manuscript. GU, YM, HM, YA, TK, KO, YH, HI, KS, KT, MM, AM, MK and ST designed the study. GU, HM, YA, TK, OK and YH acquired the data. KO, KS, HI, RO and HT wrote the 'Materials and methods' section of the manuscript. RO and HT provided technical support in performing RT-qPCR, immunohistochemical and angiogenesis assays. YM, AM, MK and ST supervised the study. All authors read and approved the final manuscript and are equally responsible for all aspects of the study, ensuring the integrity and accuracy of all parts of the study. GU and YM confirm the authenticity of all the raw data.

Ethics approval and consent to participate

All experiments were conducted according to the Guidelines for Animal Experiments of Nagoya City University Graduate School of Medicine Sciences and were approved (approval no. Medical Animal 20-020) by the Animal Care and Use Committee of the Nagoya City University Graduate School of Medical Sciences (Nagoya, Japan).

Patient consent for publication

Not applicable.

Competing interests

The authors declare that they have no competing interests.

References

1. Siegel RL, Miller KD and Jemal A: Cancer statistics, 2020. CA Cancer J Clin 70: 7-30, 2020.
2. Bray F, Ferlay J, Soerjomataram I, Siegel RL, Torre LA and Jemal A: Global cancer statistics 2018: GLOBOCAN estimates of incidence and mortality worldwide for 36 cancers in 185 countries. CA Cancer J Clin 68: 394-424, 2018.
3. Siegel RL, Miller KD and Jemal A: Cancer statistics, 2019. CA Cancer J Clin 69: 7-34, 2019.
4. GBD 2017 Pancreatic Cancer Collaborators: The global, regional, and national burden of pancreatic cancer and its attributable risk factors in 195 countries and territories, 1990-2017: A systematic analysis for the global burden of disease study 2017. Lancet Gastroenterol Hepatol 4: 934-947, 2019.
5. Rahib L, Smith BD, Aizenberg R, Rosenzweig AB, Fleshman JM and Matrisian LM: Projecting cancer incidence and deaths to 2030: The unexpected burden of thyroid, liver, and pancreas cancers in the United States. Cancer Res 74: 2913-2921, 2014.
6. Vincent A, Herman J, Schulick R, Hruban RH and Goggins M: Pancreatic cancer. Lancet 378: 607-620, 2011.
7. Klein AP, Brune KA, Petersen GM, Goggins M, Tersmette AC, Offerhaus GJA, Griffin C, Cameron JL, Yeo CJ, Kern S and Hruban RH: Prospective risk of pancreatic cancer in familial pancreatic cancer kindreds. Cancer Res 64: 2634-2638, 2004.
8. Wolpin BM, Chan AT, Hartge P, Chanock SJ, Kraft P, Hunter DJ, Giovannucci EL and Fuchs CS: ABO blood group and the risk of pancreatic cancer. J Natl Cancer Inst 101: 424-431, 2009.

9. Yoo C, Hwang JY, Kim JE, Kim TW, Lee JS, Park DH, Lee SS, Seo DW, Lee SK, Kim MH, *et al*: A randomised phase II study of modified FOLFIRI.3 vs modified FOLFOX as second-line therapy in patients with gemcitabine-refractory advanced pancreatic cancer. Br J Cancer 101: 1658-1663, 2009.

10. Oettle H, Riess H, Stieler JM, Heil G, Schwaner I, Seraphin J, Görner M, Mölle M, Greten TF, Lakner V, *et al*: Second-line oxaliplatin, folinic acid, and fluorouracil versus folinic acid and fluorouracil alone for gemcitabine-refractory pancreatic cancer: Outcomes from the CONKO-003 trial. J Clin Oncol 32: 2423-2429, 2014.

11. Katsuda M, Miyazawa M, Ojima T, Katanuma A, Hakamada K, Sudo K, Asahara S, Endo I, Ueno M, Hara K, *et al*: A double-blind randomized comparative clinical trial to evaluate the safety and efficacy of dendritic cell vaccine loaded with WT1 peptides (TLP0-001) in combination with S-1 in patients with advanced pancreatic cancer refractory to standard chemotherapy. Trials 20: 242, 2019.

12. Ioka T, Ueno M, Ueno H, Park JO, Chang HM, Sasahira N, Kanai M, Chung IJ, Ikeda M, Nakamori S, *et al*: TAS-118 (S-1 plus leucovorin) versus S-1 in patients with gemcitabine-refractory advanced pancreatic cancer: A randomised, open-label, phase 3 study (GRAPE trial). Eur J Cancer 106: 78-88, 2019.

13. Zhang Q, Lenardo MJ and Baltimore D: 30 Years of NF-κB: A blossoming of relevance to human pathobiology. Cell 168: 37-57, 2017.

14. Taniguchi K and Karin M: NF-κB, inflammation, immunity and cancer: Coming of age. Nat Rev Immunol 18: 309-324, 2018.

15. Matsuo Y, Sawai H, Ochi N, Yasuda A, Sakamoto M, Takahashi H, Funahashi H, Takeyama H and Guha S: Proteasome inhibitor MG132 inhibits angiogenesis in pancreatic cancer by blocking NF-kappaB activity. Dig Dis Sci 55: 1167-1176, 2010.

16. Itakura J, Ishiwata T, Friess H, Fujii H, Matsumoto Y, Büchler MW and Korc M: Enhanced expression of vascular endothelial growth factor in human pancreatic cancer correlates with local disease progression. Clin Cancer Res 3: 1309-1316, 1997.

17. Shi Q, Le X, Abbruzzese JL, Peng Z, Qian CN, Tang H, Xiong Q, Wang B, Li XC and Xie K: Constitutive Sp1 activity is essential for differential constitutive expression of vascular endothelial growth factor in human pancreatic adenocarcinoma. Cancer Res 61: 4143-4154, 2001.

18. Shi Q, Abbruzzese JL, Huang S, Fidler IJ, Xiong Q and Xie K: Constitutive and inducible interleukin 8 expression by hypoxia and acidosis renders human pancreatic cancer cells more tumorigenic and metastatic. Clin Cancer Res 5: 3711-3721, 1999.

19. Matsuo Y, Ochi N, Sawai H, Yasuda A, Takahashi H, Funahashi H, Takeyama H, Tong Z and Guha S: CXCL8/IL-8 and CXCL12/SDF-1alpha co-operatively promote invasiveness and angiogenesis in pancreatic cancer. Int J Cancer 124: 853-861, 2009.

20. Matsuo Y, Sawai H, Funahashi H, Takahashi H, Sakamoto M, Yamamoto M, Okada Y, Hayakawa T and Manabe T: Enhanced angiogenesis due to inflammatory cytokines from pancreatic cancer cell lines and relation to metastatic potential. Pancreas 28: 344-352, 2004.

21. Matsuo Y, Sawai H, Ochi N, Yasuda A, Takahashi H, Funahashi H, Takeyama H and Guha S: Interleukin-1alpha secreted by pancreatic cancer cells promotes angiogenesis and its therapeutic implications. J Surg Res 153: 274-281, 2009.

22. Gupta SC, Kim JH, Prasad S and Aggarwal BB: Regulation of survival, proliferation, invasion, angiogenesis, and metastasis of tumor cells through modulation of inflammatory pathways by nutraceuticals. Cancer Metastasis Rev 29: 405-434, 2010.

23. Roshak A, Jackson JR, Chabot-Fletcher M and Marshall LA: Inhibition of NFkappaB-mediated interleukin-1beta-stimulated prostaglandin E2 formation by the marine natural product Hymenialdisine. J Pharmacol Exp Ther 283: 955-961, 1997.

24. Breton JJ and Chabot-Fletcher MC: The natural product Hymenialdisine inhibits interleukin-8 production in U937 cells by inhibition of nuclear factor-kappaB. J Pharmacol Exp Ther 282: 459-466, 1997.

25. Livak KJ and Schmittgen TD: Analysis of relative gene expression data using real-time quantitative PCR and the 2(-Delta Delta C(T)) method. Methods 25: 402-408, 2001.

26. Kanda Y: Investigation of the freely available easy-to-use software 'EZR' for medical statistics. Bone Marrow Transplant 48: 452-458, 2013.

27. Aggarwal BB: Nuclear factor-kappaB: The enemy within. Cancer Cell 6: 203-208, 2004.

28. Shi Q, Le X, Wang B, Abbruzzese JL, Xiong Q, He Y and Xie K: Regulation of vascular endothelial growth factor expression by acidosis in human cancer cells. Oncogene 20: 3751-3756, 2001.

29. Xiong HQ, Abbruzzese JL, Lin E, Wang L, Zheng L and Xie K: NF-kappaB activity blockade impairs the angiogenic potential of human pancreatic cancer cells. Int J Cancer 108: 181-188, 2004.

30. Li Q, Yang G, Feng M, Zheng S, Cao Z, Qiu J, You L, Zheng L, Hu Y, Zhang T and Zhao Y: NF-κB in pancreatic cancer: Its key role in chemoresistance. Cancer Lett 421: 127-134, 2018.

31. Arlt A and Schäfer H: NFkappaB-dependent chemoresistance in solid tumors. Int J Clin Pharmacol Ther 40: 336-347, 2002.

32. Sebens S, Arlt A and Schäfer H: NF-kappaB as a molecular target in the therapy of pancreatic carcinoma. Recent Results Cancer Res 177: 151-164, 2008.

33. Holcomb B, Yip-Schneider M and Schmidt CM: The role of nuclear factor kappaB in pancreatic cancer and the clinical applications of targeted therapy. Pancreas 36: 225-235, 2008.

34. Folkman J: Angiogenesis and angiogenesis inhibition: An overview. EXS 79: 1-8, 1997.

35. Chen D, Frezza M, Schmitt S, Kanwar J and Dou QP: Bortezomib as the first proteasome inhibitor anticancer drug: Current status and future perspectives. Curr Cancer Drug Targets 11: 239-253, 2011.

36. Tsuboi K, Matsuo Y, Shamoto T, Shibata T, Koide S, Morimoto M, Guha S, Sung B, Aggarwal BB, Takahashi H and Takeyama H: Zerumbone inhibits tumor angiogenesis via NF-κB in gastric cancer. Oncol Rep 31: 57-64, 2014.

37. Aggarwal BB, Van Kuiken ME, Iyer LH, Harikumar KB and Sung B: Molecular targets of nutraceuticals derived from dietary spices: Potential role in suppression of inflammation and tumorigenesis. Exp Biol Med (Maywood) 234: 825-849, 2009.

38. Harikumar KB, Sung B, Tharakan ST, Pandey MK, Joy B, Guha S, Krishnan S and Aggarwal BB: Sesamin manifests chemopreventive effects through the suppression of NF-kappa B-regulated cell survival, proliferation, invasion, and angiogenic gene products. Mol Cancer Res 8: 751-761, 2010.

39. Omi K, Matsuo Y, Ueda G, Aoyama Y, Kato T, Hayashi Y, Imafuji H, Saito K, Tsuboi K, Morimoto M, *et al*: Escin inhibits angiogenesis by suppressing interleukin-8 and vascular endothelial growth factor production by blocking nuclear factor-κB activation in pancreatic cancer cell lines. Oncol Rep 45: 55, 2021.

40. Saito K, Matsuo Y, Imafuji H, Okubo T, Maeda Y, Sato T, Shamoto T, Tsuboi K, Morimoto M, Takahashi H, *et al*: Xanthohumol inhibits angiogenesis by suppressing nuclear factor-κB activation in pancreatic cancer. Cancer Sci 109: 132-140, 2018.

41. Kunnumakkara AB, Guha S, Krishnan S, Diagaradjane P, Gelovani J and Aggarwal BB: Curcumin potentiates antitumor activity of gemcitabine in an orthotopic model of pancreatic cancer through suppression of proliferation, angiogenesis, and inhibition of nuclear factor-kappaB-regulated gene products. Cancer Res 67: 3853-3861, 2007.

42. Sharma V, Lansdell TA, Jin G and Tepe JJ: Inhibition of cytokine production by Hymenialdisine derivatives. J Med Chem 47: 3700-3703, 2004.

43. Dobretsov S, Tamimi Y, Al-Kindi MA and Burney I: Screening for anti-cancer compounds in marine organisms in Oman. Sultan Qaboos Univ Med J 16: e168-e174, 2016.

44. Stipa F, Lucandri G, Limiti MR, Bartolucci P, Cavallini M, Di Carlo V, D'Amato A, Ribotta G and Stipa S: Angiogenesis as a prognostic indicator in pancreatic ductal adenocarcinoma. Anticancer Res 22: 445-449, 2002.

45. Benckert C, Thelen A, Cramer T, Weichert W, Gaebelein G, Gessner R and Jonas S: Impact of microvessel density on lymph node metastasis and survival after curative resection of pancreatic cancer. Surg Today 42: 169-176, 2012.

46. Amin Z, Theis B, Russell RC, House C, Novelli M and Lees WR: Diagnosing pancreatic cancer: The role of percutaneous biopsy and CT. Clin Radiol 61: 996-1002, 2006.

47. Annese T, Tamma R, Ruggieri S and Ribatti D: Angiogenesis in pancreatic cancer: Pre-clinical and clinical studies. Cancers (Basel) 11: 381, 2019.

48. Zhang Z, Ji S, Zhang B, Liu J, Qin Y, Xu J and Yu X: Role of angiogenesis in pancreatic cancer biology and therapy. Biomed Pharmacother 108: 1135-1140, 2018.